

The Type 1 Diabetes PhysioLab[®] Platform: a validated physiologically based mathematical model of pathogenesis in the non-obese diabetic mouse

L. Shoda,^{*} H. Kreuwel,[†] K. Gadkar,[‡]
Y. Zheng,[§] C. Whiting,[¶] M. Atkinson,^{††}
J. Bluestone,^{‡‡} D. Mathis,^{§§}
D. Young^{‡,***} and S. Ramanujan^{¶,***}

^{*}Entelos Inc., Foster City, [†]Baxter Healthcare Corporation, Westlake Village, [‡]Theranos, Palo Alto, [§]Genentech Inc. and [¶]Crescendo Bioscience, South San Francisco, [†]Department of Medicine, Stanford University School of Medicine, Stanford, ^{‡‡}Diabetes Center and Department of Medicine, University of California, San Francisco, CA, ^{††}Department of Pathology, University of Florida at Gainesville, Gainesville, FL, ^{§§}Department of Pathology, Harvard Medical School, Boston, MA, USA

Accepted for publication 2 March 2010
Correspondence: L. Shoda, Entelos Inc., 110 Marsh Drive, Foster City, CA 94404, USA.
E-mail: shoda@entelos.com

^{**}D.Y. and S.R. contributed equally to this work.

Summary

Type 1 diabetes is an autoimmune disease whose clinical onset signifies a lifelong requirement for insulin therapy and increased risk of medical complications. To increase the efficiency and confidence with which drug candidates advance to human type 1 diabetes clinical trials, we have generated and validated a mathematical model of type 1 diabetes pathophysiology in a well-characterized animal model of spontaneous type 1 diabetes, the non-obese diabetic (NOD) mouse. The model is based on an extensive survey of the public literature and input from an independent scientific advisory board. It reproduces key disease features including activation and expansion of autoreactive lymphocytes in the pancreatic lymph nodes (PLNs), islet infiltration and β cell loss leading to hyperglycaemia. The model uses ordinary differential and algebraic equations to represent the pancreas and PLN as well as dynamic interactions of multiple cell types (e.g. dendritic cells, macrophages, CD4⁺ T lymphocytes, CD8⁺ T lymphocytes, regulatory T cells, β cells). The simulated features of untreated pathogenesis and disease outcomes for multiple interventions compare favourably with published experimental data. Thus, a mathematical model reproducing type 1 diabetes pathophysiology in the NOD mouse, validated based on accurate reproduction of results from multiple published interventions, is available for *in silico* hypothesis testing. Predictive biosimulation research evaluating therapeutic strategies and underlying biological mechanisms is intended to deprioritize hypotheses that impact disease outcome weakly and focus experimental research on hypotheses likely to provide insight into the disease and its treatment.

Keywords: mathematical model, NOD mouse, pathogenesis, therapies, type 1 diabetes

Introduction

While many therapeutic strategies have prevented or cured type 1 diabetes successfully in animal models such as the non-obese diabetic (NOD) mouse, all clinical trials to date have failed to do so in human subjects, suggesting that a more complex interpretation of the animal data may be warranted. In our previous evaluation of interventions attempting to modulate disease in the NOD mouse, we found several cases where disparate responses had been observed following administration of a particular intervention [1]. Closer examination suggested that in some cases, dose, timing and treatment duration could theoretically account for discrepant efficacy observed within the NOD mouse model and/or between NOD *versus* human treatment

results, underscoring their probable importance in identifying appropriate protocols for human clinical trials. We therefore maintain that an improved understanding of how protocol parameters impact treatment efficacy can be expected to improve fundamentally our interpretation of animal results and facilitate translational efforts.

While theoretically desirable, it can be prohibitively expensive and time-consuming to optimize treatment protocols and fully explore treatment mechanisms of action in the laboratory. An alternative is to use physiologically based mathematical models to execute rapid, cost-efficient *in silico* analysis, resulting in testable predictions and recommendations for key corroborating experiments. Experimental validation of modelling predictions is expected to facilitate human studies by providing (a) a better understanding of

those protocol parameters contributing to efficacy and warranting close examination in human clinical trial design, and (b) a better understanding of which pathways must be conserved between animals and humans with respect to their relative contribution to disease pathology in order to expect animal experimental results to be predictive of human trial results. To bring such a tool to the development of type 1 diabetes therapeutics, we have developed a physiologically based mathematical model, the Type 1 Diabetes PhysioLab® platform, which reproduces type 1 diabetes pathogenesis in a NOD mouse from birth to diabetes onset, with extensive representation of the pancreas, the pancreatic lymph nodes (PLN) and the dynamic interactions and activities of multiple cell populations.

The Type 1 Diabetes PhysioLab platform employs a 'top-down' modelling approach to represent type 1 diabetes pathogenesis in the NOD mouse. In brief, this requires identification of the whole-animal or system-level behaviours which the model must reproduce (i.e. the 'top' level of modelling), as well as the biological components and mechanisms whose integrated and dynamic function generates these behaviours. Type 1 diabetes in the laboratory NOD mice is characterized typically by several months of normal blood glucose (normoglycaemia), before the onset of clinical symptoms, defined most commonly by elevated blood glucose (hyperglycaemia). Blood glucose levels are regulated by insulin release from beta cells (β cells) located in the pancreatic islets. Immune cell infiltration of the islets is initially detectable by 3–4 weeks of age and worsens progressively with time, where disease progression is correlated with a diminution in β cells. Further, autoreactive T cell priming and expansion have been documented in the draining pancreatic lymph nodes (PLN) [2]. Based on this understanding of type 1 diabetes, the Type 1 Diabetes PhysioLab platform explicitly represents islet β cells, autoimmune cells and mechanisms of activation and effector function, leading to loss of islet β cells and impaired glucose control (further details provided below). Notably, this top-down modelling approach requires explicit representation of the system-level behaviours of interest and allows variability in the parameterization of the underlying biology. This differs from a 'bottom-up' approach, which gathers and integrates all available data at a fundamental level, often providing valuable insights into pathway interactions but rarely reproducing a system-level behaviour in the early modelling endeavours. Nevertheless, the top-down approach employed here has elements of bottom-up approaches as well, as it relies heavily on protein and expression data to characterize relationships among entities and to assign mathematical values to the representation (e.g. the rate of islet β cell insulin production).

Physiologically based models such as the one described here are aimed at quantitatively integrating detailed biology across the system, and therefore comprise numerous state variables and parameters. The parameters in these large models include those reported in the literature and those

calibrated to match subsystem and/or system-level behaviours. Each unique parameterization of the model specifies one 'virtual NOD mouse', and each virtual mouse is validated by extensive comparisons of simulated responses against published data (see below). This approach focuses on finding biologically feasible parameterizations that reproduce critical behaviours, rather than on exact characterization of numerous difficult-to-measure parameters. In support of our approach focusing on behavioural validation and prediction, a recent analysis of 17 other systems biology models, some with more than 200 parameters, suggests that attention to predictive accuracy, rather than parametric precision, is critical and can provide scientific value in areas where biological relationships are characterized incompletely [3].

Other models of type 1 diabetes have provided valuable insight into disease pathogenesis or health care optimization (e.g. [4–9]). As this model was designed to support drug development, it differs from existing models in the following areas. First, our model includes multiple contributors to the pathogenic process in order to support physiologically based representation of a diverse set of therapeutic strategies. Second, we model multiple disease stages, tracking autoimmune pathogenesis from initiation through diabetes onset in order to investigate relative efficacy associated with interventions applied at different disease stages. It should be noted that the focus of our model (and most corresponding NOD mouse research) is on disease prevention or remission, not disease management. Finally, our model represents the physiologically based interactions leading to destruction of β cells, differentiating it from Archimedes, another large-scale diabetes model which includes detailed representation of metabolic responses, health care and complications, but in which disease results from a mathematical combination of epidemiological factors [8].

This paper is a biology-focused description of the Type 1 Diabetes PhysioLab platform intended to introduce the model at a level of detail appropriate for understanding its research applications. Due to its size, a full mathematical description of the entire platform is not reasonable within the body of text. However, to illustrate our modelling approach, the equations, assumptions and data sources for a key module, islet CD8⁺ T lymphocytes, are summarized in Appendix S1, along with textual explanations. Further, the full model is available freely online as a downloadable file, including all equations, parameters, references, documentation, simulated intervention experiments reproducing published protocols and their associated simulation results (Appendix S2).

Methods and results

Model design

We applied a top-down, outcomes-focused approach in developing the Type 1 Diabetes PhysioLab platform. This

Table 1. Scope of the type 1 diabetes PhysioLab platform.

System-level outputs	Biological components	System-level behaviours
Blood glucose	Blood glucose	Onset of hyperglycaemia
Islet cellularity	Pancreas	Islet infiltration
PLN cellularity	PLN	PLN expansion
	Islet β cells	Anti-CD8 response
	Autoantigens	Anti-B7.1/B7.2 response
	Dendritic cells	Exogenous IL-10 response
	Macrophages	LipCl ₂ MDP* response
	CD4 ⁺ T cells	Anti-CD3 response
	CD4 ⁺ regulatory T cells	Exogenous TGF- β response
	CD8 ⁺ T cells	Exendin-4 response
	B cells	Rapamycin response
	NK cells	Anti-IL-2 response
	Gut and associated lymphoid tissue	Anti-CD40L response

*Liposomal dichloromethylene diphosphonate (LipCl₂MDP) which targets phagocytes. IL, interleukin; NK, natural killer; PLN, pancreatic lymph nodes; TGF, transforming growth factor.

staged and iterative process included four phases: (a) design, (b) architecture, (c) internal validation and (d) external validation, with the two validation phases defined in keeping with the *Guidelines to Computer Modeling of Diabetes and Its Complications*, as written by an American Diabetes Association (ADA) Consensus Panel in 2004 [10]. In the design phase, we defined the model scope, including: (a) the system-level behaviours that the model must reproduce to characterize the disease state adequately (e.g. hyperglycaemia); (b) the biological components, functions and interactions needed to give rise to the system-level behaviours (e.g. cytotoxic CD8⁺ T lymphocytes, perforin-mediated β cell killing); and (c) the system-level behaviours against which the simulation results are compared in order to validate the virtual mouse (e.g. diabetic remission in response to anti-CD3). System-level behaviours were selected based on general agreement within the community on key disease characteristics. Major biological components were selected based on demonstrated importance in disease. For example, the inclusion of CD4⁺ T cells is supported by data demonstrating NOD mice genetically or therapeutically deficient in CD4⁺ T cells fail to progress to diabetes [11,12]. For validation, interventions were selected to probe the modelled biology vigorously, ensuring that the virtual mouse could

meet multiple constraints. More specifically, interventions were selected that:

- targeted different aspects of the biology;
- had been administered at different stages of disease progression;
- included protective, remitting, and exacerbating outcomes (collectively).

The model scope (Table 1) was based on thorough review of the public literature. It was reviewed and approved by an independent scientific advisory board appointed by the American Diabetes Association.

To provide a more detailed overview of the biology represented in the model, we describe the main model components, including their functional activities, modes of interaction and a selection of pertinent references. The complete set of references used in building and validating the model are contained within the model itself. The model simulates the quantities of the different cell populations, antigens and cytokines in the PLN and pancreatic islets (Fig. 1). The descriptions provided below reflect cellular activities in both the pancreas and PLN, except where noted.

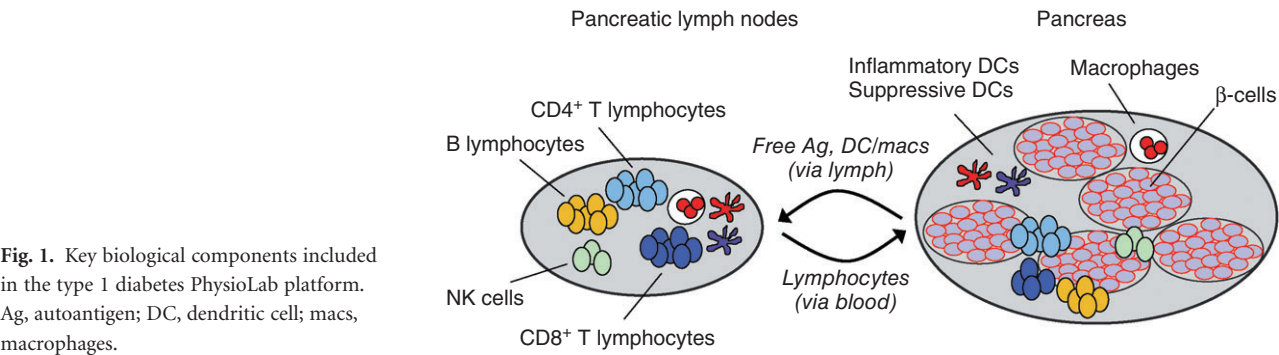


Fig. 1. Key biological components included in the type 1 diabetes PhysioLab platform. Ag, autoantigen; DC, dendritic cell; macs, macrophages.

PLN and pancreas. The PLN and pancreas are modelled as distinct tissue compartments. Interislet heterogeneity in leucocyte infiltration (i.e. co-existence of heavily, lightly and uninfected islets) and β cell destruction are well documented [13–16]. Given that this heterogeneity impacts residual β cell mass over time, we anticipated challenges in reproducing remission with a simplified representation of a single islet. Instead, 10 islets are modelled. Each islet represents a fraction (or 'bin') of the total islets in the pancreas of the NOD mouse. No islets are infiltrated at birth (at the start of a simulation), but with disease progression islets become progressively infiltrated with autoreactive immune cells, resulting in an increasing number of infiltrated islets.

Islet β cells. Each islet in the model is populated with β cells. The number of β cells, determined from β cell mass [17–20], is an outcome of developmental turnover and the level of autoimmune destruction [13,16,19,21]. β cell insulin production is regulated by the levels of glucose and inflammatory mediators [22,23].

Autoantigens. Autoantigens are modelled generically to represent several antigens identified in the literature, including insulin and glutamic acid decarboxylase [24,25]. The autoantigen level is a function of β cell mass, β cell apoptosis and insulin secretion. Autoantigens are acquired and presented on major histocompatibility complex (MHC) class I and II molecules by dendritic cells (DCs), macrophages and B lymphocytes [26–28]. β cells also present autoantigens on MHC class I molecules [29].

Dendritic cells. DCs are present in each modelled islet, even in the absence of inflammation, and recruitment of DC precursors is amplified by inflammation [30,31]. Both inflammatory and suppressive (tolerogenic) DC phenotypes are represented [32,33]. Each subset influences the developing adaptive immune response, and each has limited phagocytic capabilities [34]. DCs acquire and present antigens, produce mediators, interact with other cell types and traffic from the islets to the PLN [26,35–37].

Macrophages. Macrophages are also present in the islets even in the absence of inflammation, and recruitment of macrophage precursors is amplified by inflammation [38,39]. Macrophages perform phagocytic functions, acquire and present antigens, produce mediators, interact with other cell types and traffic to the PLN [27,37,40,41].

CD4⁺ T lymphocytes. Two groups of naive CD4⁺ T lymphocytes are represented: those specific for islet autoantigens and those specific for other antigens. This same distinction is made for all other T lymphocyte and B lymphocyte populations. In the model, thymic output of naive T cells is a specified time-dependent profile representative of what has

been observed experimentally [42–44], taking into account the relative proportion of CD4⁺ and CD8⁺ T cells [45], but is not regulated dynamically. While the intricate and highly regulated process of thymocyte development has been studied extensively, it was not included in the current model scope based on an initial focus on peripheral mechanisms of autoimmunity and tolerance. The validation protocols used to refine and test virtual mouse behaviours were dependent primarily on peripheral mechanisms. However, the model was designed to accommodate expansion of the represented biology, which could include thymocyte development.

During simulations, naive islet-autoantigen-specific (or diabetes-specific) T lymphocytes in the PLN become activated in response to autoantigen presented on MHC class II molecules and differentiate into T helper type 1 (Th1), Th2 or regulatory T cell (adaptive regulatory T cell or aT_{reg}) subsets [46–49]. Differentiated CD4⁺ T lymphocytes exert effector functions in the PLN through both contact- and soluble cytokine-mediated mechanisms and can traffic (via the circulation) to the islets [50,51]. T lymphocytes and B lymphocytes specific for other antigens are not activated in the current model.

CD4⁺ regulatory T lymphocytes. Innate (or natural) regulatory T lymphocytes (iT_{reg}), representing CD4⁺CD25⁺ T lymphocytes, are modelled as a distinct population of thymic-derived cells, distinguished from the aforementioned aT_{reg} by not requiring further differentiation to express regulatory activity [52]. Once activated via presentation of autoantigen on MHC class II molecules (MHCII antigen), regulatory T lymphocytes exhibit both cell contact-mediated and cytokine-mediated immunosuppressive activity [46,53,54].

CD8⁺ T lymphocytes. CD8⁺ T lymphocytes in the model are initially activated by MHCI-antigen in the PLN, with help provided by activated CD4⁺ T lymphocytes [55–58]. Acquired cytotoxic effector activity includes both cell contact- and cytokine-mediated mechanisms [59,60].

B lymphocytes. B lymphocytes in the model interact with DCs, natural killer (NK) cells and T lymphocytes. They differentiate (in the PLN), present antigen to CD4⁺ and CD8⁺ T lymphocytes and produce cytokines and autoantibodies [61–63]. Autoantibodies form immune complexes, influencing antigen uptake [26,64].

NK cells. On the recommendation of the scientific advisory board, NK cells were included in the model based on a high degree of scientific interest and investigation [65–68]. Because the data characterizing NK cells in type 1 diabetes and their relative role in disease are sparse relative to other cell types, the use of the NK cell module is optional (i.e. it can be omitted from the virtual mouse simulations). Inclusion of the NK cell module may be used to explore specific hypoth-

eses on the role of NK cells in disease. Activation of NK cells in the model is mediated by DCs and B lymphocytes and is regulated further by cytokines and co-stimulatory molecules [69–74]. Effector activities include cytokine synthesis and killing of immature DCs and β cells [75,76].

Blood glucose. The level of blood glucose in the model is regulated by insulin-dependent and insulin-independent mechanisms, based on deviations of insulin and glucose from their basal levels [77,78]. Dietary glucose intake is assumed to be constant and implicitly accounted for in the basal glucose level.

Gut and gut-associated lymphoid tissue. The gut and gut-associated lymphoid tissue (GALT) were built to investigate the role of local immune activity on the efficacy of oral insulin therapy. The gut tissue in the model is simplified to include only DCs. The GALT includes all the biological components present in the modelled PLN.

Model architecture

Following the design phase, the components of the model were represented mathematically. As illustrated in Fig. 2 and Appendix S1 (see end of paper), this architectural phase included laying out the biological pieces and their interactions explicitly using algebraic and ordinary differential equations in a software package (PhysioLab Modeler, Entelos Inc., Foster City, CA, USA).

Assumptions and formulation. The PLN and each islet are assumed to be well-mixed, spatially homogenous compartments. Each islet bin, as described above, contains the same model architecture. Differences in simulated behaviours in islets of different bins result from sequential and progressive lymphocyte infiltration of different islets and islet bins, leading to different degrees of accumulated infiltrate, local inflammation and damage at a given time. Common functions represented in all compartments include mediator synthesis, cellular proliferation, apoptosis and activation. Each of these functions are regulated by cell contact and soluble mediators with the following basic approach: (i) a baseline rate is assigned if data suggest a constitutive activity; (ii) additional stimulatory effects are assumed to be additive; (iii) regulators that synergize or amplify the impact of another are treated as potentiating them and represented as having multiplicative effects; (iv) inhibitory effects are represented as fractional reductions in baseline and/or stimulated effects as indicated by the data; and (v) an upper limit may be imposed, such as when the rate is proportional to the fraction of cells involved (e.g. proliferation) and saturates at 100% involvement. The likelihood of cell contact within a compartment is a function of the relative numbers of each cell type within the total cellular population. Mediator concentrations in each compartment are a function of the synthesis rate (i.e. ng/1e6

cells/h), the number of mediator-producing cells, mediator half-life and the compartment volume. Because the effect of each regulator is dependent on its concentration/activity, a standard dose–response curve was employed to describe the relationship between the regulator and its effects (Fig. 3). Published data were used to define the effective concentration range and the maximum effect. If the effective concentration range had not been published, the available data were used to define the saturating concentration and a three-log range of dose-sensitivity is assumed.

Parameterization. Parameter values were derived directly from (or calculated to be in agreement with) published data wherever quantitative data were available. Preference was given to NOD mouse data. If unavailable, data from other mouse strains, other animal species or human cells were used. The determination of the rate of tumour necrosis factor (TNF)- α synthesis by activated CD8⁺ T lymphocytes from Utsugi *et al.* [79] is a relevant illustration of data usage. They reported TNF- α production by NOD CD8⁺ T cell clones stimulated with islet cells. In all similar cases where parameters were extracted/calculated from specific literature, the references are cited in the location within the model where the parameter was used. Thus, all directly derived parameters are referenced. When direct quantitative data were unavailable, parameter values were estimated, or reverse-engineered, to fit the collective behaviour of the relevant portion of the model to available data. For example, the rate at which diabetes-specific CD8⁺ T lymphocytes are recruited into the islets is unknown. However, data were available on the relative accumulation of islet CD8⁺ T lymphocytes at various ages. Hence, the recruitment rate was estimated to yield the appropriate numbers of islet CD8⁺ T lymphocytes given the known (and modelled) expansion of CD8⁺ T lymphocytes in the PLN and levels of CD8⁺ T cell proliferation and apoptosis in the islets. Finally, after the initial parameter specification, parameters were tuned during internal validation (described below) to ensure the model reproduced pre-identified behaviours.

Model metrics. Model metrics are summarized in Table 2. To evaluate the representation of particular aspects of the biology (e.g. mathematical functional forms, parameters, associated references), researchers are directed to the full model which contains documentation on the design rationale, use of published data, assumptions, exclusions and modelling considerations.

Internal validation

To verify that the modelled biology is representative of real biology, we compared simulations against known characteristics of natural disease progression (e.g. the time-dependent accumulation of islet CD4⁺ T lymphocytes) and against reported outcomes following experimental perturbations

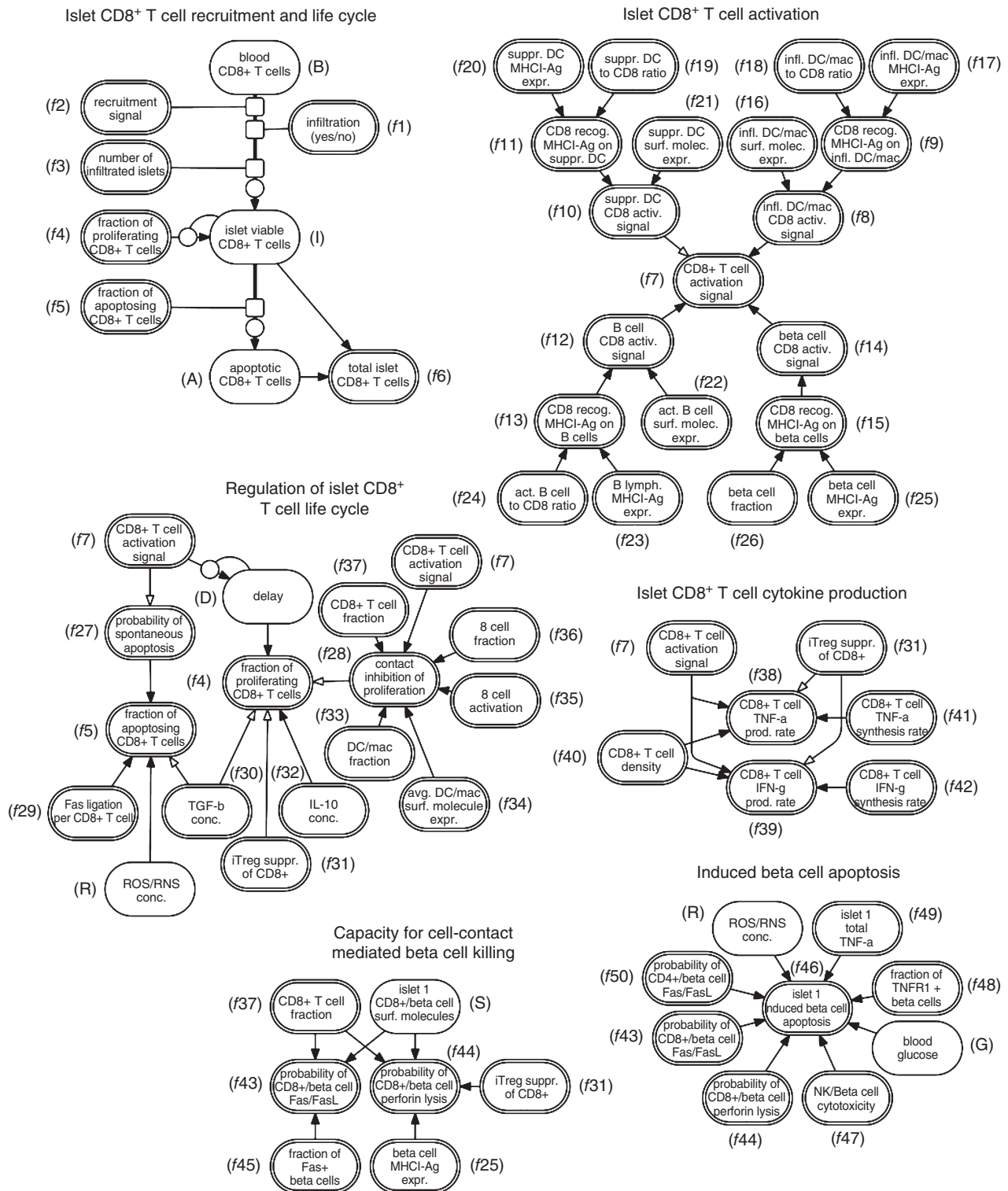


Fig. 2. The islet CD8⁺ T cell representation: cellular lifecycle, its regulation and effector activity. Ovals (nodes) represent variables; single and double border nodes represent variables determined by ordinary differential equations (ODEs) or algebraic equations, respectively. Arrows represent relationships between nodes, where closed arrows represent a positive effect and open arrows represent a negative effect.

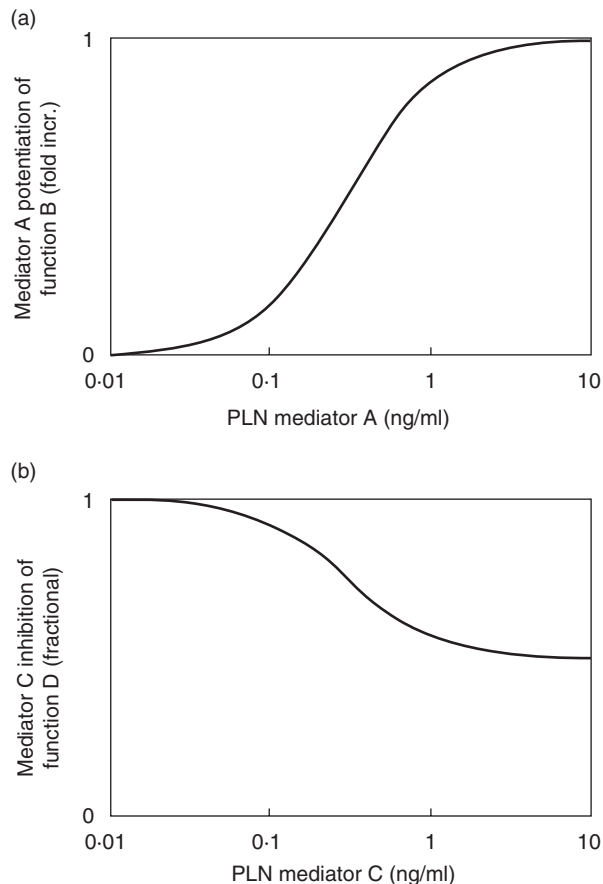


Fig. 3. Standard format describing the mathematical relationship between regulators and their effector function. (a) To represent a regulator potentiating a function, a dose–response relationship is represented, wherein the x-axis represents the dynamic range over which the regulator has the functional effect and the y-axis represents the fold increase observed in the presence of the regulator. The regulator dynamic range was defined by the literature. Where such data were lacking, the available data were assumed to represent a concentration maximum, and a three-log range was assumed. (b) To represent a regulator inhibiting a function a similar dose–response relationship is represented, wherein the y-axis represents the fractional inhibition imposed by the regulator (e.g. 50% inhibition = 0.5).

Table 2. Metrics defining the size of the type 1 diabetes PhysioLab platform.

	PLN	Islet [†]	Interventions	Systemic glucose and insulin	Systemic other [‡]
ODEs	99	89	36	14	17
Algebraic equations	353	394	390	29	109
Parameters ^{§¶}	475	754	432	25	168
Modeller comments ^{††}	544	734	215	35	58
References	792	1215	428	33	91

[†]Numbers for one representative islet ‘bin’. [‡]Includes biology outside the detailed pancreatic lymph nodes (PLN) and islet representations that is required for appropriate function of the detailed representations (e.g. thymic T cell output). [§]An additional 166 parameters are common to both the PLN and islet, e.g. macrophage interleukin (IL)-1 synthesis rate in ng/1e6 cells/h, noting that the simulated PLN *versus* islet macrophage IL-1 production may differ based on differences in cell number and modulation by cell contact and mediators. [¶]These values include both adjustable and non-adjustable parameters, the latter of which are derived typically directly from the literature, as well as initial values for all state variables. ^{††}Comments by modellers include descriptions of the biology and available literature, as well as commentary on design rationale and parameter selection. ODE, ordinary differential equations.

(e.g. protection from diabetes upon administration of anti-CD8 antibody). The objective of this internal validation phase [10] was to verify that simulations using a single set of selected parameter values (i.e. a single virtual NOD mouse) can reproduce both untreated pathogenesis and the observed disease outcomes in response to widely different interventions. The process of internal validation is also referred to commonly as ‘calibration’ or ‘training’. We use the internal validation nomenclature for consistency with the ADA guidelines for computer modelling of diabetes [10].

To compare simulation results of a single virtual NOD mouse against experimental data from NOD mouse cohorts, we established a priori standards for the comparisons. Specifically, we required this first virtual NOD mouse to be broadly representative of NOD mouse behaviours (i.e. a representative phenotype), meaning that its untreated behaviour should reflect the average behaviour reported for NOD mice, and its responses to interventions should reflect the majority response reported for each protocol (e.g. protected if diabetes incidence was reported as 10% in treated mice *versus* 90% in controls). Internal validation was then an iterative process of tuning to refine parameter values as necessary until simulation results were consistent with all pre-selected internal validation data sets (i.e. within specified ranges around reported data). Parameters selected based on parameter sensitivity analyses for outputs of interest were varied systematically within literature-derived constraints in order to meet these internal validation criteria.

Herein we present the internal validation results from the virtual NOD mouse. For comparison against features of untreated pathogenesis, we compared simulations against data on cellular expansion in the PLN, cellular infiltration and accumulation in the islets, and timing and dynamics of frank diabetes onset [13,16,30,37,80–85]. The simulated cellular profiles for CD4⁺ T lymphocytes, CD8⁺ T lymphocytes, B lymphocytes and DCs in the PLN (Fig. 4) and islets (Fig. 5) match the reported data closely. Furthermore, the untreated virtual mouse develops diabetes at 19 weeks, within the age range reported for both Taconic and The

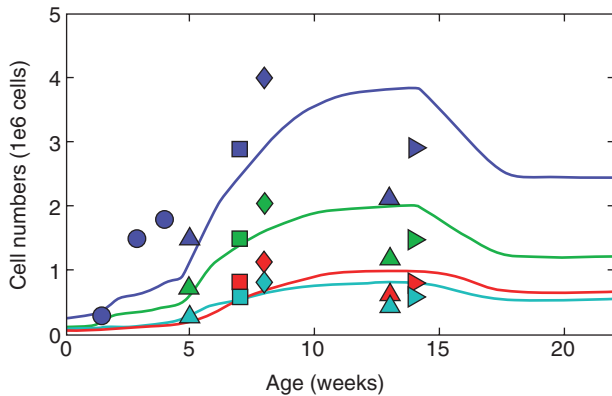


Fig. 4. Simulated pancreatic lymph nodes (PLN) cellular expansion in the virtual non-obese diabetic (NOD) mouse compares favourably with published data. Solid lines: simulation results for the virtual NOD mouse. Symbols: values derived from published data, where colour corresponds to cell type and symbols correspond to specific publications. Blue symbols: values for total leucocytes. Green symbols: values for CD4⁺ T lymphocytes. Red symbols: values for B lymphocytes. Turquoise symbols: values for CD8⁺ T lymphocytes. Circles, [37]; triangles, [80]; squares, [81]*; diamond, Kreuwel, unpublished*; side triangles, [82]*. *These papers provided total leucocyte data. The lymphocyte subsets were calculated using fractional composition data [84,109,110].

Jackson Laboratory, and with rapid loss of glycaemic control similar to experimentally observed dynamics (Fig. 6).

Meaningful constraints on the physiologically based representation are set by the requirement that a single parameterization (i.e. a virtual NOD mouse) reproduces responses to multiple and varied interventions. The simulated interventions included those targeting cell populations (anti-CD8) and cytokine activity [interleukin (IL)-10], inducing

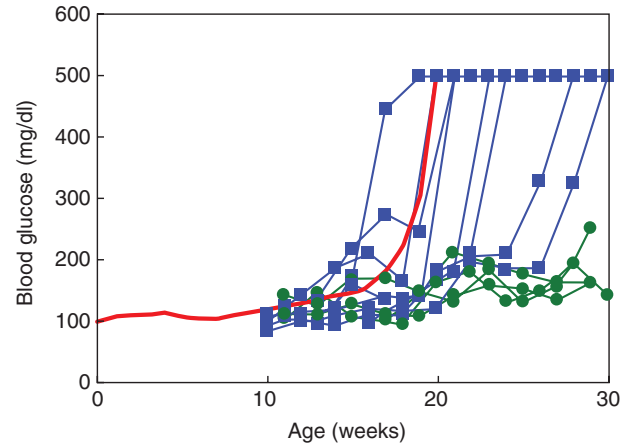
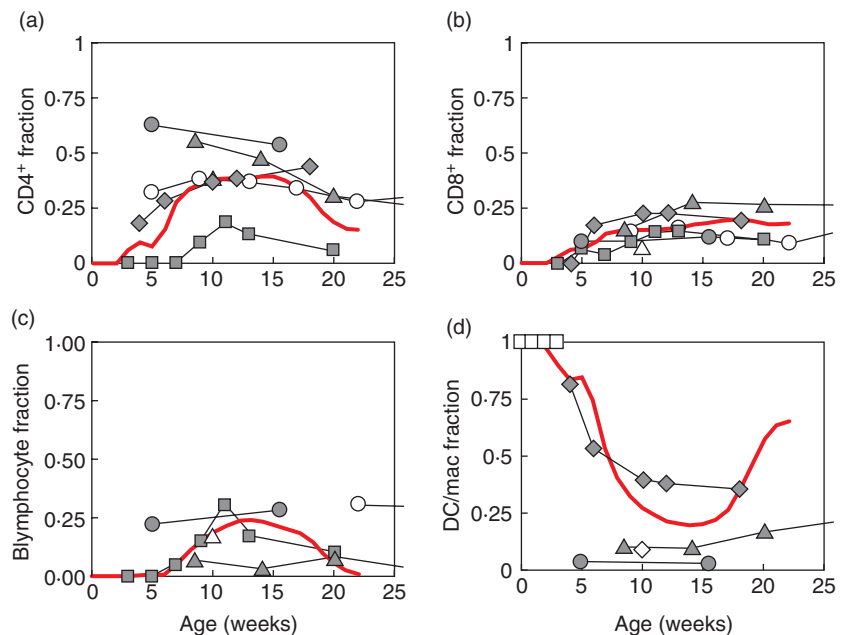


Fig. 6. Simulated glucose dynamics in the virtual non-obese diabetic (NOD) mouse compare favourably with individual NOD mouse data. Blue squares: female NOD mice that became hyperglycaemic during the study period (Kreuwel, unpublished). Green circles = female NOD mice that remained normoglycaemic during the study period (Kreuwel, unpublished). Red solid line: simulation result for the virtual NOD mouse, demonstrating onset of frank diabetes at approximately 19 weeks.

protection early but not late (liposomal dichloromethylene diphosphonate, LipCl₂MDP), exacerbating disease (anti-B7-1/B7-2) and inducing remission (anti-CD3). A pharmacokinetic (PK) and pharmacodynamic (PD) representation of each selected intervention was implemented based on public data. More specifically, model inputs included the dose, dose-frequency and timing (age) of administration. Half-lives and distribution of compounds were set to reproduce the reported serum PK. Tissue concentrations were governed by a partition coefficient, which reflected available

Fig. 5. Simulated islet leucocyte accumulation in the virtual non-obese diabetic (NOD) mouse compares favourably with published data. (a) CD4⁺ T lymphocyte fraction. (b) CD8⁺ T lymphocyte fraction. (c) B lymphocyte fraction. (d) Dendritic cell and macrophage fraction. Solid lines: simulation results for the virtual NOD mouse. Symbols: values derived from published data, where different symbols correspond to specific publications. Closed circles, [84]*; closed triangles, [13]*; closed diamonds, [30]; closed squares, [83]; open circles, [16]; open triangle, [111]; open diamond, [112]*; open squares, [31]. *For these publications, data were reported for dendritic cells (DCs) or macrophages.



data on tissue concentration of the compound and/or general properties based on molecular weight. PD was based on direct *in vivo* or *in vitro* reported effects (e.g. depletion of CD8⁺ T cells by anti-CD8). All protocols ($n = 16$ total) reporting diabetes incidence were simulated. As dictated by the internal validation objectives, the virtual NOD mouse was developed to reproduce the reported majority outcome for all intervention protocols. More specifically, parameterization of the intervention PK/PD and if necessary, the underlying biological representation were adjusted until simulations produced the desired behaviour. Parameters were adjusted only within the reported variability. While theoretically many parameters may be adjusted, at the conclusion, the virtual mouse comprises a single set of fixed parameters that reproduces faithfully biological responses to a diverse set of experimental manipulations (Table 3).

Internal validation serves as model training, and it can also provide insight into the contributions of pathogenic and regulatory pathways. For example, LipCl₂MDP, which is taken up by phagocytic cells and induces their apoptosis, has been tested at different stages of disease [86,87]. NOD mice treated with 1 mg, 1×/week from 3 to 20 weeks of age were protected (0% *versus* 80% diabetes in controls at 35 weeks). Interestingly, at 8 weeks of age, two injections of 2 mg also provided long-lasting protection (27% *versus* 100% diabetes in controls at 35 weeks), indicating that a short course of treatment modulated disease rigorously and persistently. The virtual NOD mouse recapitulates the reported majority responses (i.e. protection) for both protocols (Fig. 7a,b), providing assurance that the model represents the experimentally demonstrated importance of phagocytes in disease. Physiologically, the success of the late protocol is dependent not only on the degree of phagocyte depletion and corresponding diminution in islet infiltrates, but critically, the returning infiltrates are less cytotoxic for β cells. Phagocyte depletion provided sufficient respite to alter the cytokine milieu, skewing towards more tolerogenic DCs (Fig. 7c,d), differential expansion of regulatory T cells and the resulting persistent protection. Because the model integrates mathematically the available public data on cytokine modulation of DC function, APC and T cell interactions, T cell phenotypes and intercellular interactions (e.g. perforin-mediated β cell apoptosis), this internal validation exercise verifies not only that phagocytes are important contributors to pathogenesis at 8 weeks, but also allows the deconvolution of physiological pathways that account for the observed effects. This example illustrates how treatment outcomes verify that major pieces of the biology are contributing appropriately and also provide testable hypotheses for the details of that contribution.

External validation

To test that the internally validated virtual NOD mouse has predictive power, we compare simulations against the

reported outcomes for experimental perturbations that were not used previously during development. Because the model parameters are fixed prior to this external validation phase (i.e. no retuning to match the external validation protocol experimental results is allowed), consistency between the *in silico* and experimental results provides confidence that the virtual mouse can be used to address new research questions. The process of external validation is also referred to commonly as 'validation' or 'testing'. We use the external validation nomenclature for consistency with the ADA guidelines for computer modelling of diabetes [10].

A number of external validation interventions were identified as meeting the following requirements: (a) underlying mechanisms fall within the scope of the modelled biology; (b) interventions target different aspects of the modelled biology; and (c) protocols include variability in timing or direction of disease modulation (protection *versus* exacerbation). The implemented set of external validation interventions [exogenous transforming growth factor (TGF)- β , exendin-4, rapamycin, anti-IL-2, anti-CD40L] were selected by an independent scientific advisory board. Rapamycin illustrates the tested complexity in protocols and treatment response. Administered to pre-diabetic animals at sufficient doses, rapamycin protects from diabetes [88,89], and protection is sustained for up to 41 weeks after treatment cessation [88]. However, treatment of diabetic mice is unable to restore normoglycaemia [88]. For these same protocols, the virtual mouse recapitulates all the reported complexity, including dose-dependency, sustained effect and differential efficacy (Table 4). In another example TGF- β , a regulatory cytokine, has been shown to induce remission [90] while exendin-4, targeting β cells, was unable to restore normoglycaemia [91]. Upon simulating these same experimental conditions, diabetes remission was observed when given TGF- β but not exendin-4 (Table 4).

Similar to these examples, the virtual mouse responded to all external validation tests in a manner consistent with the majority response of real NOD mice, with the exception of a few anti-CD40L protocols (Table 4). The accurate recapitulation of multiple disease outcomes (five interventions, 21 of 24 protocols), following perturbations of distinct components of the biology and without further parameter adjustments, suggests that this virtual mouse can predict majority responses for many therapeutic strategies. The three discrepant predictions for anti-CD40L are discussed below.

Published anti-CD40L studies indicated a complex set of responses among real NOD mice (Table 4). Overall, early but not late treatment protected real NOD mice from diabetes. This trend was recapitulated successfully in the virtual NOD mouse. However, the literature also included contradictory outcomes. First, laboratory treatment of 8- to 10-week-old NOD mice with 200, 250 (two publications) or 400 μ g anti-CD40L failed to protect the majority of mice from diabetes [92–94]; in direct contrast, treatment of 8-week-old NOD mice with 250 μ g anti-CD40L protected all mice from

Table 3. Internal validation: comparison of virtual NOD mouse responses with published data.

Intervention	Protocol	Reference	Diabetes incidence (control <i>versus</i> treated) [†]	Majority outcome [‡]	Virtual mouse
α -CD8 antibody	2-week-old mice: 500 μ g, 2 \times /week for 2 weeks	[113]	87% <i>versus</i> 0% at 40 weeks	Protection by 40 weeks	Protection by 40 weeks
	12-week-old mice: 100 μ g, 1 \times /week for 20 weeks	[114]	48% <i>versus</i> 19% at 32 weeks	Protection by 32 weeks	Protection by 32 weeks
	Diabetic mice: 50 μ g, 1 \times /day for 5 days	[115]	100% <i>versus</i> 66% at 7 weeks post-onset	No remission by 7 weeks	No remission by 7 weeks
	2-week-old mice: 500 μ g, 2 \times , 1 day apart	[116]	No incidence reported, insulinitis greatly reduced at 20 weeks	–	Protection by 35 weeks
	7-week-old mice: 500 μ g, 2 \times , 1 day apart	[116]	No incidence reported, insulinitis similar to controls at 12 weeks	–	No protection by 23 weeks
α -CD3 antibody	Neonatal mice: 200 μ g single injection	[117]	75% <i>versus</i> 13% at 52 weeks	Protection by 52 weeks	Protection by 52 weeks
	4-week-old mice: 5 μ g, 1 \times /day for 5 days	[118]	73% <i>versus</i> 93% at 29 weeks	No protection by 29 weeks	No protection by 29 weeks
	8-week-old mice: 5 μ g, 1 \times /day for 5 days	[118]	73% <i>versus</i> 69% at 29 weeks	No protection by 29 weeks	No protection by 29 weeks
	12-week-old mice: 5 μ g, 1 \times /day for 5 days	[118]	85% <i>versus</i> 80% at 35 weeks	No protection by 35 weeks	No protection by 35 weeks
	Diabetic mice: 5 μ g given 1 \times /day for 5 days	[118]	100% <i>versus</i> 20% at 24 weeks post-onset [§]	Remission by 24 weeks post-onset	Remission by 24 weeks post-onset
IL-10	9-week-old mice: 1 μ g, 1 \times /day for 15 weeks	[119]	85% <i>versus</i> 25% at 28 weeks	Protection by 28 weeks	Protection by 28 weeks
	14-week-old mice: 1 μ g, 1 \times /day for 15 weeks	[119]	No effect (data not shown)	–	No protection by 19 weeks
α -B7:1 + α -B7:2 antibodies	2- to 3-week-old mice: 50 μ g, 1 \times /2 days for 14 days, one additional dose at 6–8 weeks of age	[120]	62% <i>versus</i> 94% at 23 weeks [§]	Exacerbation 4–13 weeks	Exacerbation ~6 weeks
	11.4-week-old mice: 50 μ g, 1 \times /week for 10 weeks	[120]	No effect (data not shown)	–	Exacerbation ~2 weeks
LipCl ₂ MDP	3-week-old mice: 1 mg, 1 \times /week for 17 weeks	[86]	80% <i>versus</i> 0% at 35 weeks	Protection by 35 weeks	Protection by 35 weeks
	8-week-old mice: 2 mg, 2 \times , 2 days apart	[87]	100% <i>versus</i> 27% at 35 weeks	Protection by 35 weeks	Protection by 35 weeks

[†]At the end of the study period. [‡]Majority outcome is defined as 'protection' or remission if the ratio of diabetes incidence in the treated group to that of control group is less than 0.5 at the last recorded time-point. 'Exacerbation' represents a ratio of greater than 1. [§]Results are consistent with other publications investigating treatment of non-obese diabetic (NOD) mice with anti-CD3 [103,121]. [¶]In Lenschow 1995 [120], treatment with anti-B7:1 + anti-B7:2 resulted in diabetes onset as early as 8 weeks of age, with maximum incidence of 94% by the end of the study. In contrast, control mice did not demonstrate diabetes onset until 12 weeks of age, with maximum incidence of 70% at the end of the study. The acceleration in diabetes onset was calculated between the two Kaplan–Meier curves. Comparing the times when the first mouse in each group developed diabetes (12 weeks control *versus* 8 weeks treated) yields 4 weeks acceleration. Alternatively, diabetes incidence in the control group reached 50% at 21–22 weeks of age, while the treated group achieved 50% incidence by 11 weeks of age, corresponding to 10 weeks acceleration. Finally, maximum diabetes incidence (70%) in the control group was achieved by 25 weeks of age, while the treated group achieved 68% diabetes incidence at 12 weeks of age, corresponding to 13 weeks acceleration. Overall, these comparisons suggest treatment accelerated diabetes onset by 4–13 weeks. IL, interleukin; LipCl₂MDP, liposomal dichloromethylene diphosphonate.

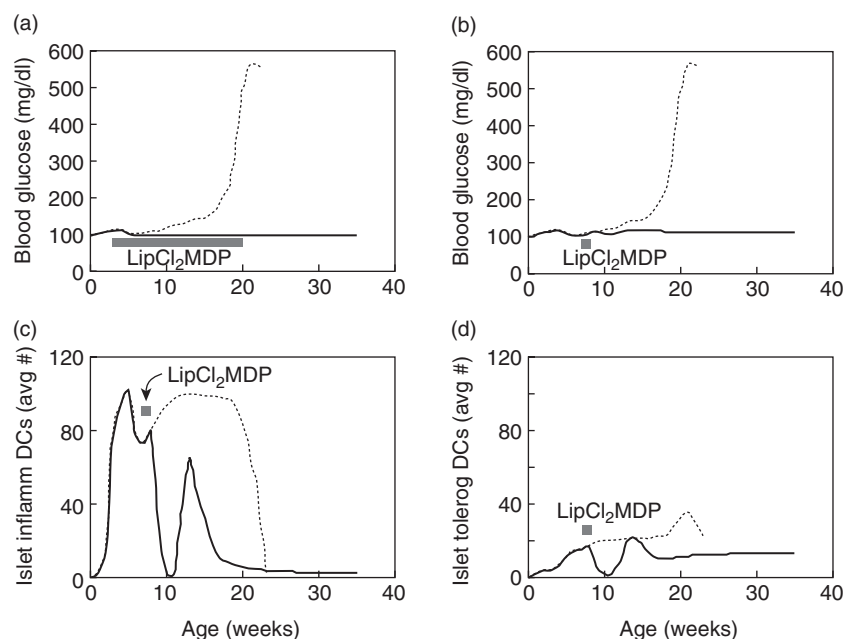


Fig. 7. Simulation results following treatment with liposomal dichloromethylene diphosphonate (LipCl₂MDP). (a) Simulated blood glucose traces are shown following treatment of the 3-week-old virtual mouse with 1 mg LipCl₂MDP 1x/week for 17 weeks as described [86]. (b) Simulated blood glucose traces are shown following treatment of the 8-week-old virtual mouse with 2 mg LipCl₂MDP 2x, 2 days apart as described [87]. Simulations run for the length of time reported in each study. (c) Analysis of simulation results following application of the 8-week protocol indicates that treatment at 8 weeks results in a precipitous decline in inflammatory dendritic cells (DCs) within infiltrated islets. Inflammatory DC numbers recover but are not sustained. (d) After *in silico* treatment at 8 weeks, suppressive/tolerogenic DCs also decline precipitously, but in the recovery phase the population is more stable than inflammatory DCs. Dotted lines: simulation results for the untreated virtual non-obese diabetic (NOD) mouse. Solid lines: simulation results for the treated virtual NOD mouse. Grey bars: duration of treatment with LipCl₂MDP as described in the above published reports.

diabetes [95]. The protocols for anti-CD40L administration were similar across all five protocols and unlikely to account for the discrepant result. Unsurprisingly, the virtual NOD mouse was not protected, consistent with four of five results.

In the second case, treatment of 3-week-old NOD mice with 100 µg or 250 µg anti-CD40L protected all treated mice from diabetes [93,96]; in contrast, treatment of 4-week-old NOD mice with approximately 400 or 500 µg reduced diabetes incidence modestly by less than 50% [92,97]. This dramatic shift in efficacy within the space of a week could reflect profound changes in the biological role of CD40L between 3 and 4 weeks, or an artificial emphasis based on interlaboratory variation in NOD mouse colonies, experimental reagents or methods. The latter seems particularly relevant, given the need to reconcile a completely efficacious low dose (100 µg) at 3 weeks and an ineffective higher dose (500 µg) at 4 weeks. The virtual NOD mouse was protected by anti-CD40L administered at 3 or 4 weeks of age, but additional investigations indicate that anti-CD40L mediated efficacy was lost at 4 weeks given minor variations in dose or disease stage [98]. Importantly, these *in silico* investigations could be used to design experiments distinguishing between the two explanations above.

In summary, the virtual NOD mouse was built to reproduce untreated pathogenesis and responses to interventions

(internal validation). The virtual NOD mouse also predicted most responses accurately to interventions not used in model construction (external validation). In the few instances where the virtual NOD mouse did not match the reported therapeutic response, a closer examination highlighted potential conflicts within the published data, in some cases providing a basis for clarifying laboratory experiments. The model as described is ready for *in silico* research. It can be updated to accommodate new data or to address additional biology not currently within the model scope. Model updates may include new validation tests to ensure that the modifications are consistent with the reported biology.

Discussion

The Type 1 Diabetes PhysioLab platform is a physiologically based mathematical model of type 1 diabetes pathogenesis in a NOD mouse, designed to facilitate type 1 diabetes research and accelerate development of human therapies. The model has a graphical user interface and incorporates much of the known biology in the PLN and islets, which sets the stage for its use as an educational and research tool to illustrate complex biological relationships at these important sites. Because data are used to define qualitatively or quantitatively the biological relationships that are embedded in the model,

Table 4. External validation: comparison of the published results of type 1 diabetes intervention protocols and simulation results from a representative virtual non-obese diabetic (NOD) mouse.

Intervention	Protocol	Reference	Diabetes incidence (control <i>versus</i> treated) [†]	Majority outcome [‡]	Virtual mouse
TGF- β	9-week-old mice: 200 μ g pCMV-TGF- β 1, 1 \times /2 week for 22 weeks	[122]	100% <i>versus</i> 42% at 32 weeks	Protection by 32 weeks	Protection by 32 weeks
Exendin-4	Diabetic mice: 5 \times 10 ⁵ PU Ad-hTGF β (insulin)	[90]	100% <i>versus</i> 33% at 16 weeks post-onset	Remission by 16 weeks post-onset	Remission by 16 weeks post-onset
	Diabetic mice: 12 nmol/kg, 1 \times /day for 4 days, repeated 4 days later	[91]	100% <i>versus</i> 100% at 17 wk post-treatment	No remission by 17 weeks post-treatment	No remission by 17 weeks post-treatment
	8-week-old mice: 6 mg/kg, 3 \times /week for 16 weeks	[88]	67% <i>versus</i> 0% at 24 weeks	Protection by 24 weeks	Protection by 24 weeks
	8-week-old mice: 12 mg/kg 3 \times /week for 16 weeks	[88]	67% <i>versus</i> 0% at 24 weeks	Protection by 24 weeks	Protection by 24 weeks
Rapamycin	9-week-old mice: 6 mg/kg, 3 \times /week for 16 weeks	[88]	60% <i>versus</i> 0% at 66 weeks	Protection by 66 weeks	Protection by 66 weeks
	9-week-old mice: 0.6 mg/kg, 3 \times /week for 16 weeks	[88]	60% <i>versus</i> 40% at 66 weeks	No protection by 66 weeks	No protection by 66 weeks
	9-week-old mice: 0.06 mg/kg, 3 \times /week for 16 weeks	[88]	60% <i>versus</i> 60% at 25 weeks	No protection by 25 weeks	No protection by 25 weeks
	10-week-old mice: 1 mg/kg, 1 \times /day for 23 weeks	[89]	100% <i>versus</i> 50% at 46 weeks	Protection by 46 weeks	Protection by 46 weeks
	10-week-old mice: 0.1 mg/kg, 1 \times /day for 23 weeks	[89]	100% <i>versus</i> 70% at 46 weeks	No protection by 46 weeks	No protection by 46 weeks
	12-week-old mice: 1 mg/kg, 1 \times /day for 23 weeks	[123]	65% <i>versus</i> 33% at 35 weeks	No protection by 35 weeks	No protection by 35 wk
	12-week-old mice: 0.1 mg/kg, 1 \times /day for 23 weeks	[123]	65% <i>versus</i> 50% at 35 weeks	No protection by 35 weeks	No protection by 35 weeks
	Diabetic mice: 6 mg/kg, 3 \times /week	[88]	No remission 5–6 weeks post-treatment	–	No remission by 5–6 weeks post-treatment
Anti-IL-2	10-day-old mice: 1 mg, repeated at day 20	[124]	12% <i>versus</i> 50% at 20 weeks [§]	Exacerbation ~9 weeks	Exacerbation ~9 weeks
	2-week-old mice: 200 μ g, 1 \times /day for 6 days	[125]	60% <i>versus</i> 100% at 30 weeks [§]	Exacerbation 3–10 weeks	Exacerbation ~9 weeks
Anti-CD40L	3-week-old mice: 250 μ g, 1 \times /2 day for 6 days, and at 6, 9, 12 weeks	[93]	80% <i>versus</i> 0% at 31 weeks	Protection by 31 weeks	Protection by 31 weeks
	3-week-old mice: 100 μ g, 1 \times /week for 2 weeks	[96]	75% <i>versus</i> 0% at 24 weeks	Protection by 24 weeks	Protection by 24 weeks
	4-week-old mice: 500 μ g, 2 \times /week for 6 weeks	[97]	73% <i>versus</i> 43% at 52 weeks	No protection by 52 weeks	Protection by 52 weeks
	4-week-old mice: 20 mg/kg, 1 \times /week for 5 weeks	[92]	80% <i>versus</i> 76% at 52 weeks	No protection by 52 weeks	Protection by 52 weeks
	8-week-old mice: 10 mg/kg, 1 \times /2 day for 6 days	[92]	83% <i>versus</i> 76% at 52 weeks	No protection by 52 weeks	No protection by 52 weeks
	8-week-old mice: 20 mg/kg, 1 \times /week for 5 weeks	[92]	83% <i>versus</i> 76% at 52 weeks	No protection by 52 weeks	No protection by 52 weeks
	8-week-old mice: 250 μ g on 0, 2, 4, and 6 days	[95]	80% <i>versus</i> 0% at 28 weeks	Protection by 28 weeks	No protection by 28 weeks
	9-week-old mice: 250 μ g, 1 \times /2 day for 6 days and at 12 weeks	[93]	100% <i>versus</i> 67% at 29 weeks	No protection by 29 weeks	No protection by 29 weeks
	10-week-old mice: 250 μ g, on 0, 2, 4, 6 and 10 days	[94]	63% <i>versus</i> 35% at 33 weeks	No protection by 33 weeks	No protection by 33 weeks

[†]At the end of the study period. [‡]Majority outcome is defined as 'protection' or 'remission' if the ratio of diabetes incidence in the treated group to that of the control group is less than or equal to 0.5 at the last recorded time-point. 'Exacerbation' represents a ratio greater than 1. [§]In Setoguchi 2005 [124], treatment with anti-interleukin (IL)-2 resulted in diabetes onset as early as 8 weeks of age, with maximum incidence of 50% at the end of the study. In contrast, control mice did not demonstrate diabetes onset until 16 weeks of age, with maximum incidence of 12% at the end of the study. The acceleration in diabetes onset was calculated between the two Kaplan–Meier curves. Comparing the times when the first mouse in each group developed diabetes (16 weeks control *versus* 8 weeks treated) yields 8 weeks acceleration. Alternatively, diabetes incidence in the control group reached its maximum (12%) at 18 weeks of age, while the anti-IL-2 group achieved 12% incidence by 8 weeks of age. This corresponds to a 10-week acceleration. Overall, these two comparisons suggest treatment accelerated diabetes onset by approximately 9 weeks. [¶]In Fujihira 2000 [125], treatment with anti-IL-2 resulted in diabetes onset as early as 14 weeks of age, with maximum incidence of 100% at the end of the study. In contrast, control mice did not demonstrate diabetes onset until 17 weeks of age, with maximum incidence of 60% at the end of the study. The acceleration in diabetes onset was calculated between the two Kaplan–Meier curves. Comparing the times when the first mouse in each group developed diabetes (17 weeks control *versus* 14 weeks treated) yields 3 weeks acceleration. Alternatively, diabetes incidence in the control group reached 50% at 26 weeks of age, while the anti-IL-2 group achieved 50% incidence by 17 weeks of age, corresponding to 9 weeks acceleration. Finally, maximum diabetes incidence (60%) in the control group was achieved by 28 weeks of age, while the anti-IL-12 group achieved 63% diabetes incidence at 18 weeks of age, corresponding to 10 weeks acceleration. Overall, these comparisons suggest treatment accelerated diabetes onset by 3–10 weeks. TGF, transforming growth factor.

the model can also be used as a data archive or continuing repository. Beyond these applications, the model simulates the represented biology, providing a mathematically integrated description which is consistent with published experimental data. Generating this description was an intensive and iterative process, which refined our understanding and interpretation of the published literature. For example, the initial modelling exercise did not include the representation of a distinct tolerogenic DC phenotype. With the initial representation, late and transient LipCl₂MDP-mediated depletion of macrophages and DCs reduced the cellular infiltrate and delayed disease onset but did not provide sustained protection despite the presence of T_{reg} cells. Briefly, when LipCl₂MDP was cleared from the system, phagocyte populations recovered and re-established a diabetogenic environment and a corresponding destructive cellular infiltrate. With no data to suggest a direct effect of LipCl₂MDP on T_{reg} cell populations, the next plausible scenario was an effect mediated through phagocytes. The representation of tolerogenic DCs was based largely on data from outside the NOD mouse literature (e.g. [99–101]), and included regulation by cytokines and cell contact. With these cells and their regulation represented explicitly, it was then possible to reproduce the published result of sustained protection with the reported level of phagocyte depletion. Importantly, simulated LipCl₂MDP depletes inflammatory DCs and tolerogenic DCs with equal potency, with sustained protection arising through the dynamic regulation of these DC subsets under conditions of reduced inflammation. The up-regulation of tolerogenic DCs also contribute to the simulated anti-CD3 mediated efficacy in diabetic NOD mice [102], which is again characterized by the return of an apparently benign cellular infiltrate [103]. In the case of anti-CD3, other mechanisms (e.g. induction of regulatory T cells) also contribute to sustained remission. The decision to represent a tolerogenic DC phenotype illustrates how the broader immunology state-of-knowledge was brought to bear in reconciling NOD mouse results with the reported underlying biology. Conversely, it illustrates a gap in understanding based on available NOD mouse data and an area where additional data on NOD DCs could clarify the mechanistic underpinnings of these therapies.

By selecting internal validation experiments that targeted different biological components, the virtual mouse was fine-tuned along multiple biological axes, yielding a single parameterization that reproduces a wide array of behaviours. By itself, this was a non-trivial and insightful exercise. Furthermore, external validation experiments were selected to assess the virtual mouse response to distinct stimuli, thereby indicating whether fine-tuning is a necessary prerequisite in the simulation of an appropriate response. The virtual mouse reproduced outcomes accurately for 21 of 24 experiments, representing five interventions. This generally positive result suggests that the virtual mouse could be a valuable counterpart to experimental investigations into

novel therapeutic strategies (assuming the main mechanisms of action are within the scope of the modelled biology). The mismatches highlighted disparities in the published anti-CD40L data set that we had not appreciated previously. However, the potential importance of dose and timing to outcomes, which were observed in the simulations, is entirely consistent with their importance in the experimental data, as highlighted in our 2004 review [1]. The model could, plausibly, be used to design experiments to reconcile disparate data. Additionally, dose/timing sensitivity argues that research efforts should use virtual mice whose disease progression (e.g. timing of diabetes onset) is aligned with the experimental mice and should evaluate a range of doses/timing to account for variability inherent in the data (i.e. NOD mouse colonies with variability in rate of disease progression) used to generate the model.

While this model is intended to broadly support research efforts in the field of type 1 diabetes, like any other model it has limitations. It does not include all biology described as contributing to pathogenesis, such as thymocyte development and neuronal regulation (e.g. [104,105]). Further, some simplifications were made to the represented biology (e.g. pooled antigen and diabetogenic T cells). Some key areas, most notably the underlying biology post-diabetes-onset, are not well characterized in the literature. There are clearly technical, financial and ethical challenges associated with studying post-diabetic NOD mice but, if we presume that lessons learned in the NOD mouse can inform human clinical trials, then these studies remain an area of critical interest. Finally, ongoing research in the NOD mouse and in the broader immunology community provides additional data that can and should be incorporated into the model. While acknowledging all the limitations described herein, it should be noted that they can be addressed through continuing model updates. At the outset of every *in silico* research project, the needs of the project are assessed against the current model to define the required model updates.

Future directions

Through grants, collaborative *in silico* and laboratory research is currently being conducted, including identification of key mechanisms driving the *Idd9* phenotype and protocol optimization for anti-CD3 plus oral insulin combination therapies, as well as nasal insulin peptide monotherapy [106–108]. It is our intention to publish the results of these research efforts which provide both *in silico* predictions and the associated experimental corroboration or refutation.

We have shown simulation results for a single virtual mouse to illustrate our design and validation methodology. To address the observed variability in NOD mouse behaviour, research using this model includes the simulated responses of a cohort of virtual mice, expressing extensive parameter variability. The approach includes applying a sys-

tematic sensitivity analysis to identify those parameters that affect simulation outcomes most strongly and varying these key parameters to produce alternate virtual mice. Alternate virtual mice may respond differently to a novel treatment strategy, just as individual NOD mice do, but importantly, researchers know how each virtual mouse is different and use that information to understand the mechanisms underlying response variability.

The Type 1 Diabetes PhysioLab Platform is intended to facilitate research design and interpretation in the scientific community. We anticipate collaborating with researchers on projects that integrate *in silico* and wet-laboratory capabilities. These could include, for example, protocol optimization for novel therapeutic strategies, delineation of therapeutic mechanisms of action, physiologically based reconciliation of apparently contradictory results and investigation into basic NOD mouse biology. We hope that the ability to rapidly predict the impact of alternate research hypotheses on disease outcomes *in silico* will streamline diabetes research, ultimately facilitating the development of preventative or curative therapies.

Acknowledgements

The development of this model was funded by the American Diabetes Association. The authors thank other members of the independent scientific advisory board (George Eisenbarth, Aldo Rossini) for input and critical review. The scientific advisory board has no financial ties to Entelos. We appreciate the scientific expertise shared by Decio Eizirik, David Serreze and Matthias von Herrath during model development. We would also like to thank Jason Chan for valuable comments.

Disclosure

L.S. is an employee of Entelos Inc. None of the other authors have conflicts of interest to declare, or any relevant financial interest, in any company or institution that might benefit from this publication.

References

- Shoda LK, Young DL, Ramanujan S *et al.* A comprehensive review of interventions in the NOD mouse and implications for translation. *Immunity* 2005; **23**:115–26.
- Anderson MS, Bluestone JA. The NOD mouse: a model of immune dysregulation. *Annu Rev Immunol* 2005; **23**:447–85.
- Gutenkunst RN, Waterfall JJ, Casey FP, Brown KS, Myers CR, Sethna JP. Universally sloppy parameter sensitivities in systems biology models. *PLoS Comput Biol* 2007; **3**:1871–8.
- Freiesleben DB, Bak P, Pociot F, Karlens AE, Nerup J. Onset of type 1 diabetes: a dynamical instability. *Diabetes* 1999; **48**:1677–85.
- Trudeau JD, Dutz JP, Arany E, Hill DJ, Fieldus WE, Finegood DT. Neonatal beta-cell apoptosis: a trigger for autoimmune diabetes? *Diabetes* 2000; **49**:1–7.
- O'Brien BA, Fieldus WE, Field CJ, Finegood DT. Clearance of apoptotic beta-cells is reduced in neonatal autoimmune diabetes-prone rats. *Cell Death Differ* 2002; **9**:457–64.
- Maree AF, Komba M, Dyck C, Labecki M, Finegood DT, Edelstein-Keshet L. Quantifying macrophage defects in type 1 diabetes. *J Theor Biol* 2005; **233**:533–51.
- Eddy DM, Schlessinger L. Archimedes: a trial-validated model of diabetes. *Diabetes Care* 2003; **26**:3093–101.
- Bergman RN. Orchestration of glucose homeostasis: from a small acorn to the California oak. *Diabetes* 2007; **56**:1489–501.
- Guidelines for computer modeling of diabetes and its complications. *Diabetes Care* 2004; **27**:2262–5.
- Shizuru JA, Taylor-Edwards C, Banks BA, Gregory AK, Fathman CG. Immunotherapy of the nonobese diabetic mouse: treatment with an antibody to T-helper lymphocytes. *Science* 1988; **240**:659–62.
- Mora C, Wong FS, Chang CH, Flavell RA. Pancreatic infiltration but not diabetes occurs in the relative absence of MHC class II-restricted CD4 T cells: studies using NOD/CIITA-deficient mice. *J Immunol* 1999; **162**:4576–88.
- Calafiore R, Pietropaolo M, Basta G, Falorni A, Picchio ML, Brunetti P. Pancreatic beta-cell destruction in non-obese diabetic mice. *Metabolism* 1993; **42**:854–9.
- Debussche X, Lormeau B, Boitard C, Toubanc M, Assan R. Course of pancreatic beta cell destruction in prediabetic NOD mice: a histomorphometric evaluation. *Diabetes Metab* 1994; **20**:282–90.
- Miyazaki A, Hanafusa T, Yamada K *et al.* Predominance of T lymphocytes in pancreatic islets and spleen of pre-diabetic non-obese diabetic (NOD) mice: a longitudinal study. *Clin Exp Immunol* 1985; **60**:622–30.
- Signore A, Pozzilli P, Gale EA, Andreani D, Beverley PC. The natural history of lymphocyte subsets infiltrating the pancreas of NOD mice. *Diabetologia* 1989; **32**:282–9.
- Bock T, Pakkenberg B, Buschard K. Genetic background determines the size and structure of the endocrine pancreas. *Diabetes* 2005; **54**:133–7.
- Hettiarachchi KD, Zimmet PZ, Myers MA. Transplacental exposure to bafilomycin disrupts pancreatic islet organogenesis and accelerates diabetes onset in NOD mice. *J Autoimmun* 2004; **22**:287–96.
- Sreenan S, Pick AJ, Levisetti M, Baldwin AC, Pugh W, Polonsky KS. Increased beta-cell proliferation and reduced mass before diabetes onset in the nonobese diabetic mouse. *Diabetes* 1999; **48**:989–96.
- Finegood DT, Scaglia L, Bonner-Weir S. Dynamics of beta-cell mass in the growing rat pancreas. Estimation with a simple mathematical model. *Diabetes* 1995; **44**:249–56.
- O'Brien BA, Harmon BV, Cameron DP, Allan DJ. Apoptosis is the mode of beta-cell death responsible for the development of IDDM in the nonobese diabetic (NOD) mouse. *Diabetes* 1997; **46**:750–7.
- Linn T, Schneider K, Goke B, Federlin K. Glucagon-like peptide-1 (7–36) amide improves glucose sensitivity in beta-cells of NOD mice. *Acta Diabetol* 1996; **33**:19–24.
- Thomas HE, Darwiche R, Corbett JA, Kay TW. Interleukin-1 plus gamma-interferon-induced pancreatic beta-cell dysfunction is mediated by beta-cell nitric oxide production. *Diabetes* 2002; **51**:311–16.
- Tisch R, Yang XD, Singer SM, Liblau RS, Fugger L, McDevitt HO. Immune response to glutamic acid decarboxylase correlates with insulinitis in non-obese diabetic mice. *Nature* 1993; **366**:72–5.

- 25 Nakayama M, Abiru N, Moriyama H *et al.* Prime role for an insulin epitope in the development of type 1 diabetes in NOD mice. *Nature* 2005; **435**:220–3.
- 26 Regnault A, Lankar D, Lacabanne V *et al.* Fcγ receptor-mediated induction of dendritic cell maturation and major histocompatibility complex class I-restricted antigen presentation after immune complex internalization. *J Exp Med* 1999; **189**:371–80.
- 27 Kovacsics-Bankowski M, Clark K, Benacerraf B, Rock KL. Efficient major histocompatibility complex class I presentation of exogenous antigen upon phagocytosis by macrophages. *Proc Natl Acad Sci USA* 1993; **90**:4942–6.
- 28 Wykes M, Pombo A, Jenkins C, MacPherson GG. Dendritic cells interact directly with naive B lymphocytes to transfer antigen and initiate class switching in a primary T-dependent response. *J Immunol* 1998; **161**:1313–19.
- 29 Thomas HE, Parker JL, Schreiber RD, Kay TW. IFN-γ action on pancreatic beta cells causes class I MHC up-regulation but not diabetes. *J Clin Invest* 1998; **102**:1249–57.
- 30 Dahlen E, Dawe K, Ohlsson L, Hedlund G. Dendritic cells and macrophages are the first and major producers of TNF-α in pancreatic islets in the nonobese diabetic mouse. *J Immunol* 1998; **160**:3585–93.
- 31 Charre S, Rosmalen JG, Pelegri C *et al.* Abnormalities in dendritic cell and macrophage accumulation in the pancreas of nonobese diabetic (NOD) mice during the early neonatal period. *Histol Histopathol* 2002; **17**:393–401.
- 32 Rothe H, Kolb H. The APC1 concept of type 1 diabetes. *Autoimmunity* 1998; **27**:179–84.
- 33 Akbari O, DeKruyff RH, Umetsu DT. Pulmonary dendritic cells producing IL-10 mediate tolerance induced by respiratory exposure to antigen. *Nat Immunol* 2001; **2**:725–31.
- 34 Kiama SG, Cochand L, Karlsson L, Nicod LP, Gehr P. Evaluation of phagocytic activity in human monocyte-derived dendritic cells. *J Aerosol Med* 2001; **14**:289–99.
- 35 Poligone B, Weaver DJ Jr, Sen P, Baldwin AS Jr, Tisch R. Elevated NF-κB activation in nonobese diabetic mouse dendritic cells results in enhanced APC function. *J Immunol* 2002; **168**:188–96.
- 36 Feili-Hariri M, Morel PA. Phenotypic and functional characteristics of BM-derived DC from NOD and non-diabetes-prone strains. *Clin Immunol* 2001; **98**:133–42.
- 37 Turley S, Poirot L, Hattori M, Benoist C, Mathis D. Physiological beta cell death triggers priming of self-reactive T cells by dendritic cells in a type-1 diabetes model. *J Exp Med* 2003; **198**:1527–37.
- 38 Reddy S, Liu W, Elliott RB. Distribution of pancreatic macrophages preceding and during early insulinitis in young NOD mice. *Pancreas* 1993; **8**:602–8.
- 39 Reddy S, Wu D, Swinney C, Elliott RB. Immunohistochemical analyses of pancreatic macrophages and CD4 and CD8 T cell subsets prior to and following diabetes in the NOD mouse. *Pancreas* 1995; **11**:16–25.
- 40 O'Brien BA, Huang Y, Geng X, Dutz JP, Finegood DT. Phagocytosis of apoptotic cells by macrophages from NOD mice is reduced. *Diabetes* 2002; **51**:2481–8.
- 41 Fan H, Longacre A, Meng F *et al.* Cytokine dysregulation induced by apoptotic cells is a shared characteristic of macrophages from nonobese diabetic and systemic lupus erythematosus-prone mice. *J Immunol* 2004; **172**:4834–43.
- 42 Scollay RG, Butcher EC, Weissman IL. Thymus cell migration. Quantitative aspects of cellular traffic from the thymus to the periphery in mice. *Eur J Immunol* 1980; **10**:210–18.
- 43 Tough DF, Sprent J. Life span of naive and memory T cells. *Stem Cells* 1995; **13**:242–9.
- 44 Tanchot C, Rocha B. Peripheral selection of T cell repertoires: the role of continuous thymus output. *J Exp Med* 1997; **186**:1099–106.
- 45 Dai Z, Lakkis FG. Cutting edge: secondary lymphoid organs are essential for maintaining the CD4, but not CD8, naive T cell pool. *J Immunol* 2001; **167**:6711–15.
- 46 Gregori S, Giarratana N, Smioldo S, Adorini L. Dynamics of pathogenic and suppressor T cells in autoimmune diabetes development. *J Immunol* 2003; **171**:4040–7.
- 47 Koarada S, Wu Y, Olshansky G, Ridgway WM. Increased nonobese diabetic Th1:Th2 (IFN-γ:IL-4) ratio is CD4+ T cell intrinsic and independent of APC genetic background. *J Immunol* 2002; **169**:6580–7.
- 48 Zhou W, Zhang F, Aune TM. Either IL-2 or IL-12 is sufficient to direct Th1 differentiation by nonobese diabetic T cells. *J Immunol* 2003; **170**:735–40.
- 49 Hoglund P, Mintern J, Waltzinger C, Heath W, Benoist C, Mathis D. Initiation of autoimmune diabetes by developmentally regulated presentation of islet cell antigens in the pancreatic lymph nodes. *J Exp Med* 1999; **189**:331–9.
- 50 Tisch R, Wang B, Atkinson MA, Serreze DV, Friedline R. A glutamic acid decarboxylase 65-specific Th2 cell clone immunoregulates autoimmune diabetes in nonobese diabetic mice. *J Immunol* 2001; **166**:6925–36.
- 51 Chen C, Lee WH, Yun P, Snow P, Liu CP. Induction of autoantigen-specific Th2 and Tr1 regulatory T cells and modulation of autoimmune diabetes. *J Immunol* 2003; **171**:733–44.
- 52 Boden E, Tang Q, Bour-Jordan H, Bluestone JA. The role of CD28 and CTLA4 in the function and homeostasis of CD4+CD25+ regulatory T cells. *Novartis Found Symp* 2003; **252**:55–63.
- 53 Bour-Jordan H, Salomon BL, Thompson HL, Szot GL, Bernhard MR, Bluestone JA. Costimulation controls diabetes by altering the balance of pathogenic and regulatory T cells. *J Clin Invest* 2004; **114**:979–87.
- 54 Tang Q, Henriksen KJ, Bi M *et al.* *In vitro*-expanded antigen-specific regulatory T cells suppress autoimmune diabetes. *J Exp Med* 2004; **199**:1455–65.
- 55 Albert ML, Jegathesan M, Darnell RB. Dendritic cell maturation is required for the cross-tolerization of CD8+ T cells. *Nat Immunol* 2001; **2**:1010–17.
- 56 Behrens GM, Li M, Davey GM *et al.* Helper requirements for generation of effector CTL to islet beta cell antigens. *J Immunol* 2004; **172**:5420–6.
- 57 Lu Z, Yuan L, Zhou X, Sotomayor E, Levitsky HI, Pardoll DM. CD40-independent pathways of T cell help for priming of CD8(+) cytotoxic T lymphocytes. *J Exp Med* 2000; **191**:541–50.
- 58 Santamaria P. Kinetic evolution of a diabetogenic CD8+ T cell response. *Ann NY Acad Sci* 2003; **1005**:88–97.
- 59 Verdager J, Schmidt D, Amrani A, Anderson B, Averill N, Santamaria P. Spontaneous autoimmune diabetes in monoclonal T cell nonobese diabetic mice. *J Exp Med* 1997; **186**:1663–76.
- 60 Amrani A, Verdager J, Anderson B, Utsugi T, Bou S, Santamaria P. Perforin-independent beta-cell destruction by diabetogenic CD8(+) T lymphocytes in transgenic nonobese diabetic mice. *J Clin Invest* 1999; **103**:1201–9.
- 61 Wheat W, Kupfer R, Gutches DG *et al.* Increased NF-κB activity in B cells and bone marrow-derived dendritic cells from NOD mice. *Eur J Immunol* 2004; **34**:1395–404.

- 62 Dustin LB, Bullock ED, Hamada Y, Azuma T, Loh DY. Antigen-driven differentiation of naive Ig-transgenic B cells *in vitro*. *J Immunol* 1995; **154**:4936–49.
- 63 Fillatreau S, Sweeney CH, McGeachy MJ, Gray D, Anderton SM. B cells regulate autoimmunity by provision of IL-10. *Nat Immunol* 2002; **3**:944–50.
- 64 Machy P, Serre K, Leserman L. Class I-restricted presentation of exogenous antigen acquired by Fcγ receptor-mediated endocytosis is regulated in dendritic cells. *Eur J Immunol* 2000; **30**:848–57.
- 65 Johansson SE, Hall H, Bjorklund J, Hoglund P. Broadly impaired NK cell function in non-obese diabetic mice is partially restored by NK cell activation *in vivo* and by IL-12/IL-18 *in vitro*. *Int Immunol* 2004; **16**:1–11.
- 66 Ogasawara K, Hamerman JA, Hsin H *et al*. Impairment of NK cell function by NKG2D modulation in NOD mice. *Immunity* 2003; **18**:41–51.
- 67 Poulton LD, Smyth MJ, Hawke CG *et al*. Cytometric and functional analyses of NK and NKT cell deficiencies in NOD mice. *Int Immunol* 2001; **13**:887–96.
- 68 Shultz LD, Schweitzer PA, Christianson SW *et al*. Multiple defects in innate and adaptive immunologic function in NOD/LtSz-scid mice. *J Immunol* 1995; **154**:180–91.
- 69 Fernandez NC, Lozier A, Flament C *et al*. Dendritic cells directly trigger NK cell functions: cross-talk relevant in innate anti-tumor immune responses *in vivo*. *Nat Med* 1999; **5**:405–11.
- 70 Nandi D, Gross JA, Allison JP. CD28-mediated costimulation is necessary for optimal proliferation of murine NK cells. *J Immunol* 1994; **152**:3361–9.
- 71 Martin-Fontecha A, Assarsson E, Carbone E, Karre K, Ljunggren HG. Triggering of murine NK cells by CD40 and CD86 (B7-2). *J Immunol* 1999; **162**:5910–16.
- 72 Diefenbach A, Jamieson AM, Liu SD, Shastri N, Raulet DH. Ligands for the murine NKG2D receptor: expression by tumor cells and activation of NK cells and macrophages. *Nat Immunol* 2000; **1**:119–26.
- 73 Hunter CA, Timans J, Pisacane P *et al*. Comparison of the effects of interleukin-1 α, interleukin-1 β and interferon-γ-inducing factor on the production of interferon-γ by natural killer. *Eur J Immunol* 1997; **27**:2787–92.
- 74 Laouar Y, Sutterwala FS, Gorelik L, Flavell RA. Transforming growth factor-β controls T helper type 1 cell development through regulation of natural killer cell interferon-γ. *Nat Immunol* 2005; **6**:600–7.
- 75 Arase H, Arase N, Saito T. Interferon γ production by natural killer (NK) cells and NK1.1+ T cells upon NKR-P1 cross-linking. *J Exp Med* 1996; **183**:2391–6.
- 76 Vitale M, Della CM, Carlomagno S *et al*. NK-dependent DC maturation is mediated by TNFα and IFNγ released upon engagement of the Nkp30 triggering receptor. *Blood* 2005; **106**:566–71.
- 77 Bergman RN, Ider YZ, Bowden CR, Cobelli C. Quantitative estimation of insulin sensitivity. *Am J Physiol* 1979; **236**:E667–77.
- 78 Topp B, Promislow K, deVries G, Miura RM, Finegood DT. A model of beta-cell mass, insulin, and glucose kinetics: pathways to diabetes. *J Theor Biol* 2000; **206**:605–19.
- 79 Utsugi T, Yoon JW, Park BJ *et al*. Major histocompatibility complex class I-restricted infiltration and destruction of pancreatic islets by NOD mouse-derived beta-cell cytotoxic CD8+ T-cell clones *in vivo*. *Diabetes* 1996; **45**:1121–31.
- 80 Friedline RH, Wong CP, Steeber DA, Tedder TF, Tisch R. I-selectin is not required for T cell-mediated autoimmune diabetes. *J Immunol* 2002; **168**:2659–66.
- 81 Beaudoin L, Laloux V, Novak J, Lucas B, Lehuen A. NKT cells inhibit the onset of diabetes by impairing the development of pathogenic T cells specific for pancreatic beta cells. *Immunity* 2002; **17**:725–36.
- 82 Laloux V, Beaudoin L, Jeske D, Carnaud C, Lehuen A. NK T cell-induced protection against diabetes in V α14-J α281 transgenic nonobese diabetic mice is associated with a Th2 shift circumscribed regionally to the islets and functionally to islet autoantigen. *J Immunol* 2001; **166**:3749–56.
- 83 Jarpe AJ, Hickman MR, Anderson JT, Winter WE, Peck AB. Flow cytometric enumeration of mononuclear cell populations infiltrating the islets of Langerhans in prediabetic NOD mice: development of a model of autoimmune insulinitis for type I diabetes. *Reg Immunol* 1990; **3**:305–17.
- 84 Faveeuw C, Gagnerault MC, Lepault F. Expression of homing and adhesion molecules in infiltrated islets of Langerhans and salivary glands of nonobese diabetic mice. *J Immunol* 1994; **152**:5969–78.
- 85 Yu L, Robles DT, Abiru N *et al*. Early expression of anti-insulin autoantibodies of humans and the NOD mouse: evidence for early determination of subsequent diabetes. *Proc Natl Acad Sci USA* 2000; **97**:1701–6.
- 86 Jun HS, Yoon CS, Zbytniuk L, van Rooijen N, Yoon JW. The role of macrophages in T cell-mediated autoimmune diabetes in nonobese diabetic mice. *J Exp Med* 1999; **189**:347–58.
- 87 Nikolic T, Geutskens SB, van Rooijen N, Drexhage HA, Leenen PJ. Dendritic cells and macrophages are essential for the retention of lymphocytes in (peri)-insulinitis of the nonobese diabetic mouse: a phagocyte depletion study. *Lab Invest* 2005; **85**:487–501.
- 88 Baeder WL, Sredy J, Sehgal SN, Chang JY, Adams LM. Rapamycin prevents the onset of insulin-dependent diabetes mellitus (IDDM) in NOD mice. *Clin Exp Immunol* 1992; **89**:174–8.
- 89 Rabinovitch A, Suarez-Pinzon WL, Shapiro AM, Rajotte RV, Power R. Combination therapy with sirolimus and interleukin-2 prevents spontaneous and recurrent autoimmune diabetes in NOD mice. *Diabetes* 2002; **51**:638–45.
- 90 Luo X, Yang H, Kim IS *et al*. Systemic transforming growth factor-β1 gene therapy induces foxp3+ regulatory cells, restores self-tolerance, and facilitates regeneration of beta cell function in overtly diabetic nonobese diabetic mice. *Transplantation* 2005; **79**:1091–6.
- 91 Ogawa N, List JF, Habener JF, Maki T. Cure of overt diabetes in NOD mice by transient treatment with anti-lymphocyte serum and exendin-4. *Diabetes* 2004; **53**:1700–5.
- 92 Molano RD, Berney T, Li H *et al*. Prolonged islet graft survival in NOD mice by blockade of the CD40–CD154 pathway of T-cell costimulation. *Diabetes* 2001; **50**:270–6.
- 93 Balasa B, Krahel T, Patstone G *et al*. CD40 ligand–CD40 interactions are necessary for the initiation of insulinitis and diabetes in nonobese diabetic mice. *J Immunol* 1997; **159**:4620–7.
- 94 Nanji SA, Hancock WW, Luo B *et al*. Costimulation blockade of both inducible costimulator and CD40 ligand induces dominant tolerance to islet allografts and prevents spontaneous autoimmune diabetes in the NOD mouse. *Diabetes* 2006; **55**:27–33.
- 95 Makhoulouf L, Grey ST, Dong V *et al*. Depleting anti-CD4 monoclonal antibody cures new-onset diabetes, prevents recurrent autoimmune diabetes, and delays allograft rejection in nonobese diabetic mice. *Transplantation* 2004; **77**:990–7.

- 96 Waid DM, Vaitaitis GM, Wagner DH, Jr. Peripheral CD4^{lo}CD40⁺ auto-aggressive T cell expansion during insulin-dependent diabetes mellitus. *Eur J Immunol* 2004; **34**:1488–97.
- 97 Markees TG, Serreze DV, Phillips NE *et al.* NOD mice have a generalized defect in their response to transplantation tolerance induction. *Diabetes* 1999; **48**:967–74.
- 98 Gadkar KG, Shoda LK, Kreuwel HT *et al.* Dosing and timing effects of anti-CD40L therapy: predictions from a mathematical model of type 1 diabetes. *Ann NY Acad Sci* 2007; **1103**:63–8.
- 99 Cederbom L, Hall H, Ivars F. CD4⁺CD25⁺ regulatory T cells down-regulate co-stimulatory molecules on antigen-presenting cells. *Eur J Immunol* 2000; **30**:1538–43.
- 100 Vieira PL, de Jong EC, Wierenga EA, Kapsenberg ML, Kalinski P. Development of Th1-inducing capacity in myeloid dendritic cells requires environmental instruction. *J Immunol* 2000; **164**:4507–12.
- 101 Alpan O, Bachelder E, Isil E, Arnheiter H, Matzinger P. 'Educated' dendritic cells act as messengers from memory to naive T helper cells. *Nat Immunol* 2004; **5**:615–22.
- 102 Young DL, Ramanujan S, Kreuwel HT, Whiting CC, Gadkar KG, Shoda LK. Mechanisms mediating anti-CD3 antibody efficacy: insights from a mathematical model of type 1 diabetes. *Ann NY Acad Sci* 2006; **1079**:369–73.
- 103 Chatenoud L, Thervet E, Primo J, Bach JF. Anti-CD3 antibody induces long-term remission of overt autoimmunity in nonobese diabetic mice. *Proc Natl Acad Sci USA* 1994; **91**:123–7.
- 104 Godfrey DI, Kinder SJ, Silvera P, Baxter AG. Flow cytometric study of T cell development in NOD mice reveals a deficiency in alphabetaTCR+CD8[–] thymocytes. *J Autoimmun* 1997; **10**:279–85.
- 105 Winer S, Tsui H, Lau A *et al.* Autoimmune islet destruction in spontaneous type 1 diabetes is not beta-cell exclusive. *Nat Med* 2003; **9**:198–205.
- 106 Zheng Y, Bresson D, Fradkin M, Chan J, Von Herrath M, Whiting CC. Biosimulations predict optimal oral insulin/anti-CD3 and oral insulin/exendin-4 combination treatment regimens for the reversal of diabetes in the non-obese diabetic (NOD) mouse. *Clin Immunol* 2008; **127**:S101.
- 107 Chan J, Zheng Y, Foustier G, Von Herrath M, Whiting CC. *In silico* modeling of intranasal insulin B:9-23 peptide therapy in the non-obese diabetic (NOD) mouse: mechanisms of action, protocol optimization, and implications of clinical trial design. *Clin Immunol* 2008; **127**:S102.
- 108 Zheng Y, Kruger A, Pearson T *et al.* Integrated biosimulation and laboratory research delineates key mechanisms by which the *Idd9* locus protects from diabetes in the non-obese diabetic (NOD) mouse. *Acta Diabetol* 2007; **44**:55.
- 109 Berzins SP, Venanzi ES, Benoist C, Mathis D. T-cell compartments of prediabetic NOD mice. *Diabetes* 2003; **52**:327–34.
- 110 Greeley SA, Moore DJ, Noorchashm H *et al.* Impaired activation of islet-reactive CD4 T cells in pancreatic lymph nodes of B cell-deficient nonobese diabetic mice. *J Immunol* 2001; **167**:4351–7.
- 111 Tominaga Y, Nagata M, Yasuda H *et al.* Administration of IL-4 prevents autoimmune diabetes but enhances pancreatic insulinitis in NOD mice. *Clin Immunol Immunopathol* 1998; **86**:209–18.
- 112 Rosmalen JG, Pigman MJ, Kersseboom R, Drexhage HA, Leenen PJ, Homo-Delarche F. Sex steroids influence pancreatic islet hypertrophy and subsequent autoimmune infiltration in nonobese diabetic (NOD) and NODscid mice. *Lab Invest* 2001; **81**:231–9.
- 113 Chowdhury SA, Nagata M, Yamada K *et al.* Tolerance mechanisms in murine autoimmune diabetes induced by anti-ICAM-1/LFA-1 mAb and anti-CD8 mAb. *Kobe J Med Sci* 2002; **48**:167–75.
- 114 Sempe P, Ezine S, Marvel J *et al.* Role of CD4⁺CD45RA⁺ T cells in the development of autoimmune diabetes in the non-obese diabetic (NOD) mouse. *Int Immunol* 1993; **5**:479–89.
- 115 Mottram PL, Murray-Segal LJ, Han W, Maguire J, Stein-Oakley AN. Remission and pancreas isograft survival in recent onset diabetic NOD mice after treatment with low-dose anti-CD3 monoclonal antibodies. *Transpl Immunol* 2002; **10**:63–72.
- 116 Wang B, Gonzalez A, Benoist C, Mathis D. The role of CD8⁺ T cells in the initiation of insulin-dependent diabetes mellitus. *Eur J Immunol* 1996; **26**:1762–9.
- 117 Hayward AR, Shriber M. Reduced incidence of insulinitis in NOD mice following anti-CD3 injection: requirement for neonatal injection. *J Autoimmun* 1992; **5**:59–67.
- 118 Chatenoud L, Primo J, Bach JF. CD3 antibody-induced dominant self tolerance in overtly diabetic NOD mice. *J Immunol* 1997; **158**:2947–54.
- 119 Pennline KJ, Roque-Gaffney E, Monahan M. Recombinant human IL-10 prevents the onset of diabetes in the nonobese diabetic mouse. *Clin Immunol Immunopathol* 1994; **71**:169–75.
- 120 Lenschow DJ, Ho SC, Sattar H *et al.* Differential effects of anti-B7-1 and anti-B7-2 monoclonal antibody treatment on the development of diabetes in the nonobese diabetic mouse. *J Exp Med* 1995; **181**:1145–55.
- 121 Chatenoud L, Thervet E, Primo J, Bach JF. [Remission of established disease in diabetic NOD mice induced by anti-CD3 monoclonal antibody]. *C R Acad Sci III* 1992; **315**:225–8.
- 122 Piccirillo CA, Chang Y, Prud'homme GJ. TGF-beta1 somatic gene therapy prevents autoimmune disease in nonobese diabetic mice. *J Immunol* 1998; **161**:3950–6.
- 123 Shapiro AM, Suarez-Pinzon WL, Power R, Rabinovitch A. Combination therapy with low dose sirolimus and tacrolimus is synergistic in preventing spontaneous and recurrent autoimmune diabetes in non-obese diabetic mice. *Diabetologia* 2002; **45**:224–30.
- 124 Setoguchi R, Hori S, Takahashi T, Sakaguchi S. Homeostatic maintenance of natural Foxp3⁺ CD25⁺ CD4⁺ regulatory T cells by interleukin (IL)-2 and induction of autoimmune disease by IL-2 neutralization. *J Exp Med* 2005; **201**:723–35.
- 125 Fujihira K, Nagata M, Moriyama H *et al.* Suppression and acceleration of autoimmune diabetes by neutralization of endogenous interleukin-12 in NOD mice. *Diabetes* 2000; **49**:1998–2006.

Supporting information

Additional Supporting Information may be found in the online version of this article:

Appendix S1. Detailed illustration of modelled islet CD8⁺ T cells.

Appendix S2. A zip file that includes the T1D model, its associated software and supporting documents for their use. The downloaded zip file will contain:

- a readme.txt file listing the platform requirements for use of the software (note that the software operates in a Windows XP environment only);

- a 'Documents' folder containing two instructional pdf files on use of the software and model;
- a 'PhysioLab Viewer Installer' folder containing the installation package (double-click on the 'msi' file to install the software and model on your machine).

Please note: Wiley-Blackwell are not responsible for the content or functionality of any supporting materials supplied by the authors. Any queries (other than missing material) should be directed to the corresponding author for the article.